

Phase Transformations in Feldspar Group Minerals with Paracelsian Topology under High Temperature and High Pressure

L.A. Gorelova

Institute of Earth Sciences, St. Petersburg State University, Universitskaya nab. 7/9, St. Petersburg, 199034, Russia

Received 28 December 2022; accepted 14 February 2023

Abstract—Feldspar group minerals (feldspars) form up to 60 vol.% of the Earth’s crust. The knowledge of their stability under extreme conditions (high-pressure and high-temperature) allow to better understand the processes, that occur in the subduction and collision processes. This review focuses on the behavior of feldspars with paracelsian topology (seven mineral species: three borosilicates, two aluminosilicates and two beryllophosphates) at elevated temperatures and pressures. Partly, new data on high-temperature behavior of paracelsian $\text{BaAl}_2\text{Si}_2\text{O}_8$ (based on in situ high-temperature powder X-ray diffraction) provided. The high-temperature studies of 5 feldspar minerals with paracelsian topology (danburite, maleevite, pekovite, paracelsian, slawsonite) revealed that all of them are stable at least up to 800 °C. Among all of them only paracelsian undergoes polymorphic transition (at 930 °C), whereas all other minerals decompose or amorphisize. The structural deformations of these minerals demonstrate the different anisotropy degree upon heating, whereas the average volume expansion is similar for all of them ($\alpha_V = 23 \times 10^{-6} \text{ }^\circ\text{C}^{-1}$). High-pressure behavior was studied for six of seven minerals with paracelsian topology (danburite, maleevite, pekovite, paracelsian, slawsonite, hurlbutite). The studied minerals undergo transformations with the stepwise increasing of coordination number of frame-forming cations from 4 to 5 and 6 upon compression. The discovering of unusual structural units under extreme conditions (e.g., fivefold-coordinated polyhedral) can influence on the concentration and transport processes of trace elements that should be taken into account when interpreting geochemical and geophysical data. The crystal structure stability range of studied minerals highly depends on the chemical composition of frame-forming cations: aluminosilicates are the least stable and undergo the phase transitions below 6 GPa; borosilicates preserve their initial crystal structure up to ~20 GPa; beryllium phosphates do not undergo phase 2 transformations up to 75 GPa. It has been shown that transformations pathway of isostructural compounds highly depends on the chemical composition of both extraframework and frame-forming cations that involves the difficulties with predictions of their behavior under extreme conditions.

Keywords: feldspar; paracelsian; high pressure; high temperature; phase transition; stability

INTRODUCTION

Feldspars belong to one of the groups of the most common minerals of the Earth’s crust, that is why a great number of publications are devoted to the study of their chemical composition, crystal structure, as well as stability under various conditions. The results of these studies are summarized in large monographs and reference books; among them, it is worth mentioning several classical works (Smith and Brown, 1988; Parsons, 1994; Deer et al., 2001; Bokii and Borutzkii, 2003). Despite the fact that they have been studied in sufficient detail, feldspars are of great interest to researchers even today, as confirmed, for example, by very recent reviews (Krivovichev, 2020; Henderson 2021). However, it is worth mentioning that the vast majority of such works are devoted to the study of alkaline feldspars and plagioclases.

According to the review by S.V. Krivovichev (2020), 29 currently known mineral species can be regarded as feldspar-related, although the structures of some are very different from those of “classical” feldspars. The crystal structures of all the most common feldspars, as well as some rare ones, belong to the feldspar topology itself. In addition to this topology, there are four others, namely: paracelsian, svyatoslavite, dmisteinbergite and hollandite; the latter two differ from the feldspar topology significantly: dmisteinbergite-like minerals are layered, and the hollandite-like structures, although being framework, are formed by SiO_6 octahedra. Crystal structures of minerals with feldspar, paracelsian and svyatoslavite topologies are formed by tetrahedra, which, joining *via* vertices, form frameworks.

There are two main approaches to describe crystal structures of feldspars with the feldspar and paracelsian topologies (Smith and Rinaldi, 1962; Smith, 1978): the structure is based on (1) interconnected layers of four- and eight-membered rings of TO_4 tetrahedra ($T = \text{Si, Al, B, Be, P, Fe, Zn, As}$) (Fig. 1a); (2) “crankshaft” chains of TO_4 tetrahedra (Fig. 1b, c). The difference in the frameworks is in the dif-

✉ Corresponding author.

E-mail address: l.gorelova@spbu.ru (L.A. Gorelova)

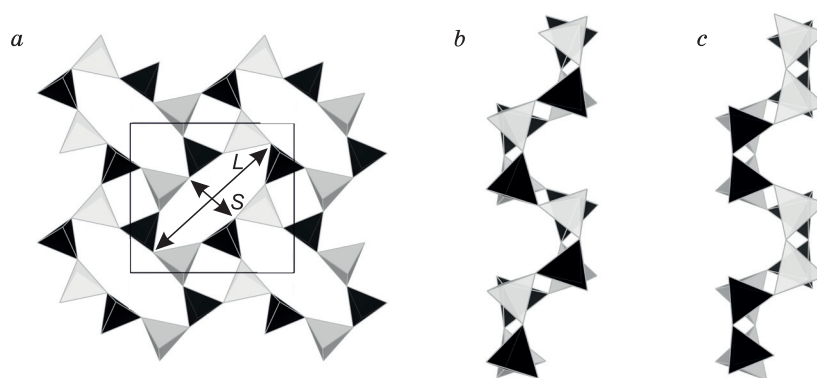


Fig. 1. The crystal structure of feldspar-related minerals with the topology of paracelsian: a layer of four- and eight-membered rings of TO_4 tetrahedra ($T = \text{Si, Al, B, Be, P}$) (a); a “crankshaft” chain of TO_4 tetrahedra ($T = \text{Si, B}$) (b) and TO_4 tetrahedra ($T = \text{Si, Al, Be, P}$) (c). Grey and black colors of coordination polyhedra indicate different types of T atoms.

ferent type of junction between the “crankshaft” chains; this leads to the fact that structures with the paracelsian topology are flexible, while the feldspar ones are rigid (Krivovichev, 2020).

This paper presents new data on the study of thermal deformations of paracelsian (in Supplementary materials), as well as summarizes the results of studies of feldspar-related minerals with paracelsian topology (FSPT) under extreme conditions (high temperatures and/or pressures), shows the stability ranges of phases with different compositions, the dependence of the transformation path of the crystal structure on the chemical composition and initial geometry.

GEOLOGICAL CONDITIONS

As it was noted earlier, the FSPT minerals are quite rare. Some of them (maleevite, pekovite and strontiohurlbutite) are currently known in the only deposit (Pautov et al., 2004; Rao et al., 2014), while others (e.g., danburite) are widespread and can be rock-forming.

The exact geneses of maleevite, $\text{BaB}_2\text{Si}_2\text{O}_8$, and pekovite, $\text{SrB}_2\text{Si}_2\text{O}_8$, have not been determined. Both minerals were found in rounded quartz lumps from the moraine of the Dara-i-Pioz glacier (Tajikistan) which contains fragments of alkaline rocks and pegmatites from the upper part of the Dara-i-Pioz massif (Pautov et al., 2004, 2022). Strontiohurlbutite, $\text{SrBe}_2\text{P}_2\text{O}_8$, was described in the Nanping granite pegmatite (China), in association with quartz, albite, muscovite, spodumene and amblygonite (Rao et al., 2014). Crystals of all three minerals do not exceed 2 mm in diameter and usually form intergrowths with other minerals, which makes their study difficult.

Paracelsian, slawsonite and hurlbutite are also quite rare, but are still known in several different deposits. Paracelsian $\text{BaAl}_2\text{Si}_2\text{O}_8$ was described in the Benallt Mine (Wales, UK) (Spencer, 1942), and in the marble quarries of Piedmont (Italy) (Tacconi, 1905), but there is no detailed description of the samples. Its strontium analogue, slawsonite $\text{SrAl}_2\text{Si}_2\text{O}_8$,

and the beryllophosphate analogue, hurlbutite $\text{CaBe}_2\text{P}_2\text{O}_8$, are slightly more widespread. Slawsonite was first described in metamorphic rocks of Oregon (USA) (Griffen et al., 1977), and later found in other deposits in the USA, Spain, Japan, Czech Republic and Canada, but their description is practically absent and published only in the form of presentations at various conferences. According to the data of D. Matýšek and J. Jirásek (2016), slawsonite is commonly found in the rocks of low metamorphism facies. Hurlbutite is known in several deposits around the world (USA, Sweden, Spain, Finland, Czech Republic and China), which are characterized by high Li and P contents (Mrose, 1952). It should be noted that the genesis of the first finding of hurlbutite is not completely understood, since it was found not in bedrock pegmatite; however, it is generally accepted that it is formed in the early stages of hydrothermal vein formation (Mrose, 1952). The most common mineral among feldspars with paracelsian topology is danburite $\text{CaB}_2\text{Si}_2\text{O}_8$; it is not only found in a large number of deposits around the world, but is also used as the ore for boron (Ratkin et al., 2018). C.U. Shepard first described danburite (1839); it is commonly found in calcareous skarns, as well as granite pegmatites, marbles, hydrothermal veins and sedimentary strata (Grew and Anovitz, 1996).

THE CONNECTION BETWEEN CHEMICAL COMPOSITION AND CRYSTAL STRUCTURE

As it was mentioned before, feldspar-related minerals with paracelsian topology include seven mineral species; three of them are borosilicates (danburite, pekovite and maleevite), two are aluminosilicates (slawsonite and paracelsian) and two are beryllophosphates (hurlbutite and strontiohurlbutite). Interestingly, all minerals with paracelsian topology contain only alkaline earth metal cations (Ca, Sr, Ba) as an extraframework cation, while minerals with feldspar topology may contain alkaline, alkaline earth cations (K, Na, Rb, Ca, Ba) or even NH_4 -groups. At the same time, among synthetic analogues of feldspars with paracelsian topology

there are compounds with feldspar topology, containing both alkaline elements, and (NH₄)- and (H₂O)- groups as extraframework cations (Klaska and Jarchow, 1977; Kimata, 1993; Zabukovec-Logar et al., 2001; Tripathi and Parise, 2002; Liu et al., 2003; Qin et al., 2009; Dordevič, 2011; Boruntea et al., 2019). The framework of all such compounds, excepting KBSi₃O₈ (Kimata, 1993), consists of a combination of TO₄ tetrahedra, typical for natural compounds (T = Al, Si, P, Be, Zn, As), with rare GaO₄ and/or GeO₄ tetrahedra.

Topological symmetry of the paracelsian framework is *Ccmm* (Smith, 1978). However, the symmetry of real compounds is lower, due to the fact that the framework is formed by two different types of atoms (Krivovichev, 2020). Minerals with paracelsian topology crystallize in two spatial groups, depending on chemical composition: *Pnma* (borosilicates) and *P2₁/c* (aluminosilicates and beryllophosphates). The orthorhombic group (*Pnma*) assumes the need of tetrahedra of the same type to connect to each other (BO₄ + BO₄ / SiO₄ + SiO₄) (Fig. 1b), while in monoclinic symmetry (*P2₁/c*) tetrahedra alternate (Fig. 1c).

It is important to note that all FSPT minerals (with the exception of the most common of them, danburite) crystallize in nature with a very small amount of impurities; that means that they are usually extremely stoichiometric. For example, maleevite and pekovite, although are found in the same deposit, do not form solid solutions (Pautov et al., 2004). According to all published chemical analyses, maleevite never includes Sr in its composition (Pautov et al., 2004; Gorelova et al., 2020); however, it may contain minor Ca and Na admixture, as well as quite significant amounts of Pb, which is typical for minerals found in the Dara-i-Pioz massif (Pautov et al., 2004). L.A. Pautov et al. (2004) found maleevite grains with a high lead content, but their size did not make it possible to describe it as a separate mineral species. Pekovite did not show lead in any of the analyses; however, it may contain minor admixtures of Ca, Ba and Na (Gorelova et al., 2020).

Danburite may contain the greatest variety of impurities among all FSPT minerals: Al, Fe²⁺, Mn, Mg, Sr, Na, Be, K, Cu, Zn, REE, Pb, etc. (Dana, 1892; Huong et al., 2016), but even the total content of admixture elements does not exceed 5 wt.%; i.e., the formula of the mineral is very close to ideal.

Aluminosilicate minerals, as well as their borosilicate analogues, do not practically contain impurities: slawsonite may contain a small amount of Ba (Tagai et al., 1995; Gorelova et al., 2021a) or Ca (Griffen et al., 1977). According to L.J. Spencer (1942), paracelsian may contain traces of Ti, Fe, Mn, Ca, Mg, Na and K, but later studies showed only minor amounts of Na and K (Chiari et al., 1985; Gorelova et al., 2021a). It is also interesting to note that the chemical compound with CaAl₂Si₂O₈ composition, although having a large number of polymorphic modifications (Gorelova et al., 2023b), does not form a structure with the paracelsian topology under either natural or synthetic conditions.

Chemical composition of hurlbutite has not been studied in detail; the discoverer of this mineral mentioned Si, Al, Na and Sr as impurities in trace amounts (Mrose, 1952). Strontiohurlbutite may contain Ba and Ca as admixtures, in quite noticeable quantities (up to 3 wt.%) (Rao et al., 2014). The same authors note that hurlbutite can contain SrO up to 10 wt.%, that means that beryllophosphate FSPT minerals can form solid solutions. It is interesting to note that to date there is no barium analogue of hurlbutite and strontiohurlbutite: the synthetic BaBe₂P₂O₈ has layered structure with the dmisteinbergite topology. However, a lead analogue of hurlbutite, PbBe₂P₂O₈, is known (Dal Bo et al., 2014), which has not been found in nature yet.

STABILITY UNDER HIGH TEMPERATURE CONDITIONS

The high-temperature evolution of the crystal structure has been studied for 5 out of 7 FSPT minerals (Table 1), namely for paracelsian (the present work, Suppl. Mat.),

Table 1. Thermal expansion coefficients ($\times 10^6 \text{ }^\circ\text{C}^{-1}$) of feldspar group minerals with the paracelsian topology along the main axes of the thermal expansion tensor, as well as along the main crystallographic axes, at different temperatures

Mineral	Formula, space group	<i>t</i> , °C	α_{11}	α_{22}	α_{33}	$\mu(\alpha_{33}^{\wedge}c)$	α_a	α_b	α_c	α_β	α_ν	References
Paracelsian	BaAl ₂ B ₂ O ₈ , <i>P2₁/c</i>	30	8	1	8	44	8	1	8	0	18	(This work)
		900	15	-1	14	31	15	-1	14	-1	28	
		30–900	12	0	11	34	12	0	11	0	23	
Slawsonite	SrAl ₂ B ₂ O ₈ , <i>P2₁/c</i>	30	6	2	8	22	7	2	8	1	17	Calculated by data (Gorelova et al., 2021b)
		900	12	4	13	35	12	3	13	1	28	
		30–900	9	3	11	28	10	3	11	1	23	
Danburite	CaB ₂ B ₂ O ₈ , <i>Pnma</i>	30	6	4	6	–	= α_{11}	= α_{22}	= α_{33}	–	16	(Sugiyama and Takéuchi, 1985; Gorelova et al., 2015)
		900	10	6	10	–	= α_{11}	= α_{22}	= α_{33}	–	26	
		30–900	9	6	9	–	= α_{11}	= α_{22}	= α_{33}	–	24	
Pekovite	SrB ₂ B ₂ O ₈ , <i>Pnma</i>	30	6	6	3	–	= α_{11}	= α_{22}	= α_{33}	–	15	(Gorelova et al., 2012, 2015)
		900	11	9	5	–	= α_{11}	= α_{22}	= α_{33}	–	25	
		30–900	9	8	4	–	= α_{11}	= α_{22}	= α_{33}	–	21	
Maleevite	BaB ₂ B ₂ O ₈ , <i>Pnma</i>	30–900	16	5	5	–	= α_{11}	= α_{22}	= α_{33}	–	26	(Gorelova et al., 2015)
<average> ₅											23	

slawsonite (Gorelova et al., 2021b), danburite, pekovite and maleevite (Sugiyama and Takéuchi, 1985; Gorelova et al., 2012, 2015). In other words, at present boro- and aluminosilicates have been studied, while both berylllophosphates have not been studied yet.

All the studied minerals are quite stable and do not undergo phase transformations up to 800–1000 °C, depending on the chemical composition (Fig. 2). The minerals containing the largest extraframework cation (Ba), i.e., maleevite and paracelsian, are the least stable and start to decompose at the temperatures of ~800 and ~930 °C, respectively (Gorelova et al., 2015; Suppl. Mat.). Maleevite decomposes with the formation of $Ba_3B_6Si_2O_{16}$, which according to the studies of the $BaO-B_2O_3-SiO_2$ system (Levin and Ugrinic, 1953), is the only stable phase of this system under ambient conditions. Paracelsian, as it was described above, does not decompose with the temperature increasing, but undergoes a polymorphic transition with the symmetry reduction from $P2_1/c$ to $I2/c$ and the formation of celsian (feldspar with the topology of feldspar), which is thermodynamically stable modification under ambient conditions.

The thermal behavior of pekovite was studied only up to 900 °C (Gorelova et al., 2012, 2015). In this temperature range, pekovite does not undergo any phase transitions. Most probably, pekovite starts to decompose with the formation of $SrSiO_3$ at the temperatures of 900–1000 °C: for our studies (Gorelova et al., 2012, 2015) we used a synthetic analogue of pekovite obtained by the method of solid-phase synthesis (900 °C/127 h), which contained insignificant amount of $SrSiO_3$; the temperature increasing up to 1000 °C led to the increase of the amount of $SrSiO_3$ (Gorelova et al., 2015). A calcium mineral, danburite, seems to be the most stable among other borosilicates and decomposes only at ~1000 °C with the formation of cristobalite and wollastonite, as well as gaseous B_2O_3 (Brun and Ghose, 1964). Data on the high-temperature behavior of the strontium analogue of paracelsian, i.e., slawsonite, are contradictory. According to T. Tagai et al. (1995) and Z. Tasaryova et al. (2014) slaw-

sonite undergoes a polymorphic transition at 320 °C; according to H.U. Bambauer and H.E. Nager (1981), and R.A. McCauley (2000) structural transformations occur at 500 or 600 °C. At the same time, the existence of phase transitions at the temperatures above 500 °C are not confirmed by the data of differential thermal analysis (Tagai et al., 1995). Our recent studies do not show any structural changes up to at least 1000 °C (Gorelova et al., 2021b).

Although there are no direct data on the stability of berylllophosphate members of the feldspar group with paracelsian topology (hurlbutite and strontiohurlbutite) upon heating, based on the fact that their synthetic analogues were obtained by the solid-state reactions at 1000 °C (Dal Bo et al., 2014), it can be assumed that they are stable at least up to this temperature. The second indirect criterion of their stability at the temperatures above 700 °C is the formation of a synthetic analogue of hurlbutite upon decomposition of hydroxylherderite, $Ca_2Be_2P_2O_8(OH)_2$ (Gorelova et al., 2023a).

Thus, thermal stability of FSPT minerals mainly depends on the size of the extraframework cation. Although the composition of the framework is less significant, it can be noted that the berylllophosphate framework is stable to higher temperatures, comparing with aluminosilicate and borosilicate, with the latter being the least stable in this series. Earlier it was noted that the formation of solid solutions is not really typical for the FSPT minerals, but the presence of isomorphous admixtures can considerably influence on the stability range of these minerals.

THE CRYSTAL STRUCTURE DEFORMATIONS UNDER HIGH-TEMPERATURE CONDITIONS

The high-temperature crystal structure deformations of danburite (at ambient pressure) were first studied by the single-crystal X-ray diffraction method (Sugiyama and Takéuchi, 1985). The authors showed that the most significant changes in the structure occur due to an elongation of one of the B–O bonds within the BO_4 tetrahedra, despite the fact that tetrahedra are usually considered to be rigid structural units (Dove et al., 1993, 2000). Later, the thermal behavior of danburite and its Sr- and Ca-analogues were investigated using the X-ray powder diffraction (Gorelova et al., 2015). According to this study, anisotropy of thermal expansion increases with the increasing of the size of the extraframework cation ($\alpha_{max}/\alpha_{min} \sim 1.5$ for danburite (Ca), ~ 2.1 for pekovite (Sr) and ~ 3.3 for maleevite (Ba)), while the average volume thermal expansion practically does not change. At the same time, the directions of maximum and minimum expansions are in the plane of the layer formed by 4- and 8-membered rings of TO_4 tetrahedra ($T = Si, B$). It was assumed that this is due to a so-called hinged mechanism of the crystal structure deformations (Sleight, 1995), where the four-membered ring of TO_4 tetrahedra ($T = Si, B$) acts as the hinge (Fig. 3).

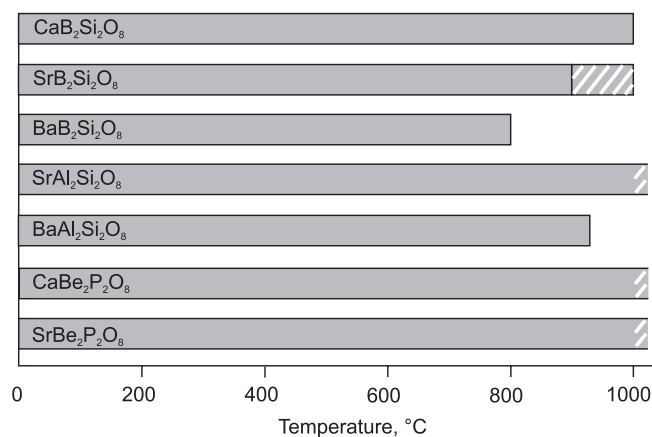


Fig. 2. Stability of feldspar-related minerals with the topology of paracelsian under high temperature.

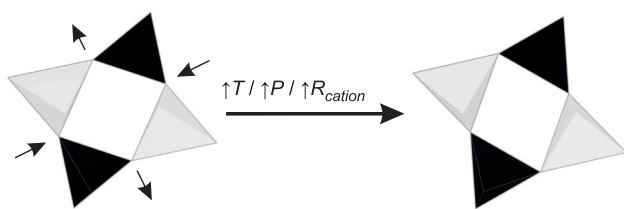


Fig. 3. Deformations of the four-membered ring of tetrahedra under changes of temperature (T), pressure (P) or size of extra-framework cation (R_{cation}). Grey and black colors of coordination polyhedra indicate different T atom types ($T = \text{Si, Al, B, Be, P}$).

Deformations of the aluminosilicate FSPT members (paracelsian and slawsonite (Gorelova et al., 2021b)) under high-temperature conditions are very similar to the deformations of borosilicates described above and are explained by the same mechanisms, but the degree of anisotropy is higher: $\alpha_{max}/\alpha_{min} \sim 3.9$ for slawsonite (Sr) and ~ 12.0 for paracelsian (Ba) (Table 1); this can be explained by the lower symmetry. Such significant difference in anisotropy of thermal expansion of paracelsian, as compared to other minerals of similar topology, can be due to the crystal structure “preparation” for a polymorphic transformation, by the analogy with layered borosilicate minerals (Krzhozhanovskaya et al., 2018).

As it was mentioned above, the increase in the size of the extraframework cation leads to the increase in the anisotropy degree of thermal expansion; this fact is confirmed by the example of boro- and aluminosilicates. Replacement of one of the framework-forming cations (B (0.11 Å) to Al (0.39 Å)) with the identical extraframework cations leads to similar changes (Table 1); this was already noted for pekovite and slawsonite (Gorelova et al., 2015, 2021b). It is interesting to note that regardless of the framework composition, the value of the average volume expansion for all FSPT minerals remains constant: $\langle \alpha_v \rangle = 23 \times 10^{-6} \text{ } ^\circ\text{C}^{-1}$ (Table 1); this indicates that the main reason defining the thermal behavior is not the chemical composition of the compound, but the type of its crystal structure.

Thus, the principal behavior of the compound is primarily determined by the framework topology. The next most important stability factor is the extraframework cation and finally – the type of the framework-forming cation. The information, provided above, can help interpret the data on the thermal behavior of isostructural compounds of variable compositions.

STABILITY UNDER HIGH PRESSURE CONDITIONS

The evolution of the crystal structure behavior under high pressure conditions (and room temperature) has been studied for all the considered FSPT minerals, except strontiohurlbutite (Pakhomova et al., 2017, 2019; Gorelova et al., 2019, 2020, 2021a).

According to the traditional crystal chemistry of silicates, the main structural unit of such compounds under ambient conditions is the SiO_4 tetrahedron, and SiO_6 octahedron under high-pressure conditions (Finger and Hazen, 2000). In this case, the SiO_4 tetrahedron is usually considered as a rigid, practically incompressible structural unit, and structural transformations are mostly explained by the changes of angles between the tetrahedra (Dove et al., 1993, 2000; Palmer et al., 1997). Similar statement is usually also correct for such close structures as alumino-, boro-, beryllsilicates, etc. These statements are correct for most compounds at pressures below 10 GPa (Angel, 1994; Downs et al., 1999; Angel et al., 2012; Mookherjee et al., 2016). Recent studies (Pakhomova et al., 2020) show that at higher pressures, the TO_4 tetrahedra can undergo significant distortions, which ultimately leads to an increase in the coordination number and the formation of the TO_5 and/or TO_6 polyhedra. Thus, even in the Earth’s upper mantle the crystal structures of minerals may contain unusual coordination groups that will affect a geochemical cycle of elements and their redistribution.

The deformation mechanism of the crystal structures of all studied FSPT minerals at relatively low pressures is the same: pressure increasing causes elongation of the eight-membered ring, numerically determined by an increase in the ratio of its long (L) and short (S) diagonals (Table 2). As the result, in the structures of danburite, paracelsian, slawsonite and hurlbutite, one or more T atoms ($T = \text{Si, Al, Be, P}$) displace so that an additional fifth oxygen atom joins to its coordination sphere (Fig. 4). Therefore, the T atom increases its coordination number to five and acquires a trigonal bipyramidal geometry (Figs. 4, 5a). At the same time, the junction of pentacoordinated polyhedra can be of two

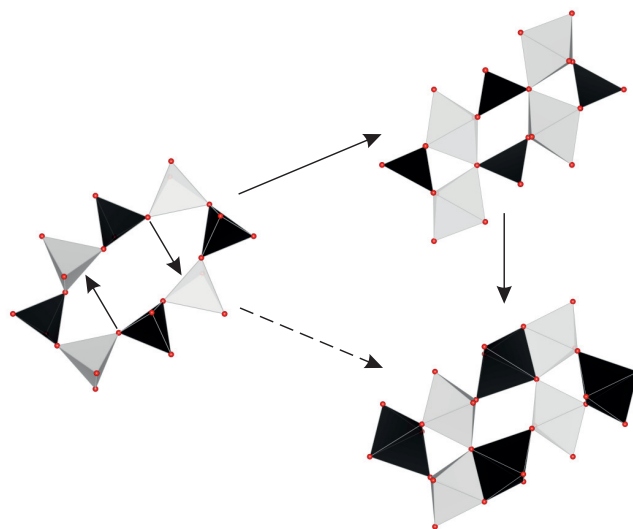


Fig. 4. The scheme of transformation of the eight-membered ring of tetrahedra under the pressure increase, with the formation of one or two types of TO_5 polyhedra ($T = \text{Si, Al, Be, P}$). Grey and black colors of coordination polyhedra indicate different T atom types, red spheres indicate oxygen atoms hereinafter.

Table 2. Quantitative characteristic of the eight-membered ring deformations in the structures of the feldspar-related minerals with the paracelsian topology, under changes in chemical composition, temperature and pressure

Diagonal	20 °C/0.0001 GPa	900 °C/0.0001 GPa	20 °C/ <i>X</i> *, GPa	ΔT	ΔP	References
<i>Paracelsian</i> BaAl ₂ Si ₂ O ₈						
L1 (long)	9.686(4)	–	9.619(6)	–	–0.067	(Gorelova et al., 2019)
S1 (short)	3.616(4)	–	3.457(6)	–	–0.159	
L2 (long)	9.672(4)	–	9.613(5)	–	–0.059	
S2 (short)	3.625(4)	–	3.463(5)	–	–0.162	
L1/S1	2.68	–	2.78	–	–	
L2/S2	2.67	–	2.78	–	–	
<i>Slawsonite</i> SrAl ₂ Si ₂ O ₈						
L1 (long)	9.676(6)	9.672(9)	9.61(6)	–0.004	–0.066	(Gorelova et al., 2020, 2021b)
S1 (short)	3.426(6)	3.465(9)	3.16(6)	0.039	–0.266	
L2 (long)	9.665(6)	9.657(8)	9.53(5)	–0.008	–0.135	
S2 (short)	3.423(6)	3.463(8)	3.23(5)	0.040	–0.193	
L1/S1	2.82	2.79	3.04	–	–	
L2/S2	2.82	2.79	2.95	–	–	
<i>Danburite</i> CaB ₂ Si ₂ O ₈						
L (long)	8.796(1)	8.819(4)	8.333(2)	0.023	–0.462	(Sugiyama and Takéushi, 1985;
S (short)	3.185(1)	3.229(4)	2.540(2)	0.044	–0.647	Gorelova et al., 2015, 2020a; Pakhomova et al., 2017)
L/S	2.76	2.73	3.28	–	–	
<i>Pekovite</i> SrB ₂ Si ₂ O ₈						
L (long)	8.772(3)	–	8.396(8)	–	–0.376	(Gorelova et al., 2020)
S (short)	3.380(3)	–	2.631(8)	–	–0.749	
L/S	2.60	–	3.19	–	–	
<i>Maleevite</i> BaB ₂ Si ₂ O ₈						
L (long)	8.627(3)	–	8.29(3)	–	–0.337	(Gorelova et al., 2020)
S (short)	3.605(3)	–	2.45(3)	–	–1.155	
L/S	2.39	–	3.38	–	–	
<i>Hurlbutite</i> CaBe ₂ P ₂ O ₈						
L1 (long)	8.999(16)	–	8.172(6)	–	–0.827	(Bakakin et al., 1974; Pakhomova et al., 2019)
S1 (short)	3.312(16)	–	2.388(7)	–	–0.924	
L2 (long)	8.941(16)	–	8.081(6)	–	–0.860	
S2 (short)	3.317(16)	–	2.443(7)	–	–0.874	
L1/S1	2.72	–	3.42	–	–	
L2/S2	2.70	–	3.31	–	–	
<i>Strontiohurlbutite</i> SrBe ₂ P ₂ O ₈						
L1 (long)	9.012(6)	–	–	–	–	(Rao et al., 2014)
S1 (short)	3.428(4)	–	–	–	–	
L2 (long)	8.993(6)	–	–	–	–	
S2 (short)	3.476(4)	–	–	–	–	
L1/S1	2.63	–	–	–	–	
L2/S2	2.59	–	–	–	–	

Note. **X*, GPa is the last measured pressure before the phase transition: 3, 6, 22, 18, 36, 67 GPa for paracelsian, slawsonite, danburite, pekovite, maleevite and hurlbutite, respectively (Fig. 1).

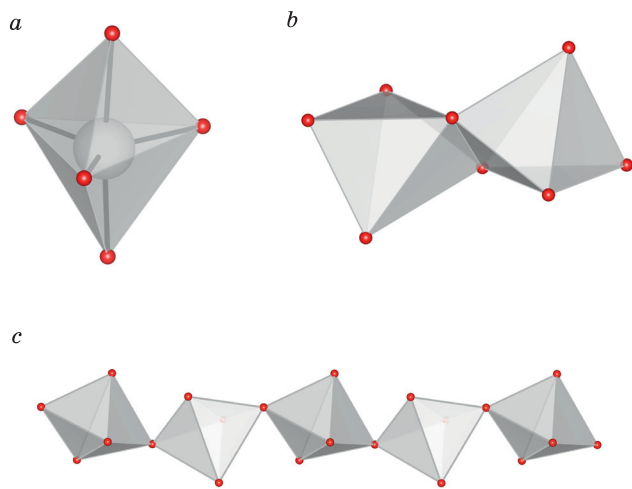


Fig. 5. Structural units of the crystal structure of feldspars with the paracelsian topology under elevated pressure: a trigonal bipyramid TO_5 ($T = \text{Si, Al, Be, P}$) (a); a T_2O_8 dimer (b); a chain of TO_5 polyhedra (c).

types: TO_5 polyhedra joining *via* vertices form chains (Fig. 5c), and the edge-sharing TO_5 polyhedra form T_2O_8 dimers (Fig. 5b).

Although maleevite and pekovite are full analogues of danburite and differ only in the size of the extraframework cation (Ba (1.38 Å) – in maleevite, Sr (1.21 Å) – in pekovite, Ca (1.06 Å) – in danburite (Shannon, 1976)), pentacoordinated silicon does not form in their high-pressure modifications (Gorelova et al., 2020). Thus, pekovite undergoes a displacement isosymmetrical phase transition at a pressure above 23 GPa, while maleevite does not have an “intermediate” modification at all (Fig. 6). Obviously, the differences in the behavior are due to the features of the extraframework cation, which significantly affects the mechanism of polymorphic transformations. It is also interesting to note that the structure of the described borosilicates becomes more stable, as the size of the extraframework cation (Ca→Sr→Ba) increases, that contradicts traditional ideas about the behavior of structurally identical compounds under high pressure conditions (Neuhaus, 1964).

Depending on the chemical composition of the framework (boro-, aluminosilicates, beryllphosphates), the transformation path of FSPT minerals also slightly differs. As a result of the reconstructive phase transition, borosilicates, regardless of the extraframework cation at a pressure above 32 GPa, form a close packing triclinic framework structure (space group $P1$) (Fig. 6), consisting of chains of SiO_6 octahedra (Fig. 7a) and B_2O_7 dimers unchanged under the pressure increase (Fig. 7b) (Pakhomova et al., 2017; Gorelova et al., 2020). All three minerals amorphize under further pressure increase. It is interesting to note that upon decompression maleevite and pekovite show slightly different results (Gorelova et al., 2020). The high-pressure modification of pekovite preserves its crystal structure up to ~12 GPa upon decompression; after that the crystal almost completely

amorphizes. In the case of maleevite, a gradual pressure decreasing leads to the formation of, apparently, two more polymorphic modifications with unknown crystal structures.

The behavior of aluminosilicate minerals is highly dependent on the extraframework cations: slawsonite (Sr) does not undergo reconstructive phase transitions, but amorphizes at pressures above 29 GPa (Gorelova et al., 2021a). A reconstructive polymorphic transition in paracelsian, $BaAl_2Si_2O_8$, at 28.5 GPa, accompanied by the symmetry increasing, as well as in the case of borosilicates, leads to the formation of a close packing structure consisting of SiO_6 and AlO_6 octahedra (Figs. 6, 8) (Gorelova et al., 2019). It is important to note that, unlike borosilicates, where SiO_6 octahedra are joined to BO_4 tetrahedra *via* vertices, polyhedra of different types (Si or Al) in paracelsian are exclusively edge-sharing. At pressures above 32 GPa, paracelsian amorphizes. Thus, for aluminosilicates with the paracelsian-type structure, as well as for similar borosilicates, the stability of the crystal structure under pressure increases with the increasing of the extraframework cation. However, it is important to note that unlike borosilicate analogues, reconstructive transitions in both aluminosilicates are reversible (Gorelova et al., 2019, 2021a).

The reconstructive transformation of beryllphosphate (hurlbutite) leads to the symmetry reduction to triclinic, as for borosilicates (Pakhomova et al., 2019), but the structural motif is completely different. The crystal structure of hurlbutite-IV consists of T ($T = \text{Be, P}$) atoms in exclusively six-fold coordination. PO_6 octahedra form complex layers in which some octahedra are edge-sharing, while the others are connected to each other *via* vertices (Figs. 6, 9).

It is important to note that despite the fact that the mechanism of deformations is the same, the formation of pentacoordinated and hexacoordinated polyhedra occurs at significantly different pressures: aluminosilicates undergo phase transitions at pressures of about 6 GPa, borosilicates – at above 20 GPa, and beryllphosphates – at above 70 GPa (Gorelova et al., 2021b). A.S. Pakhomova et al. (2020) suggest that the greater compressibility of AlO_4 tetrahedra and, as a result, the increase in the coordination number of Al at lower pressures, comparing with SiO_4 tetrahedra, is explained by their lower ionic potential (the ratio of ion charge to ionic radius (Shannon, 1976)): 7.7 for Al^{3+} and 15.4 for Si^{4+} . Similarly, we can explain the fact that the coordination number of boron (ionic potential for $B^{3+} = 27.3$) does not increase in borosilicates upon compression. However, the beryllphosphate mineral hurlbutite, as it was noted above, undergoes the first phase transition at a significantly higher pressure (> 75 GPa) (Pakhomova et al., 2019), whereas the ionic potentials of $Be^{2+} = 7.4$ and $P^{5+} = 16.1$ are very close to those of Al and Si, respectively. Therefore, we need other mechanisms to explain the reasons for this variety of polymorphic modifications in isostructural modifications.

Based on the obtained results, beryllphosphates are the most stable among isostructural minerals at high pressures (and ambient temperature), while boro- and aluminosilicates

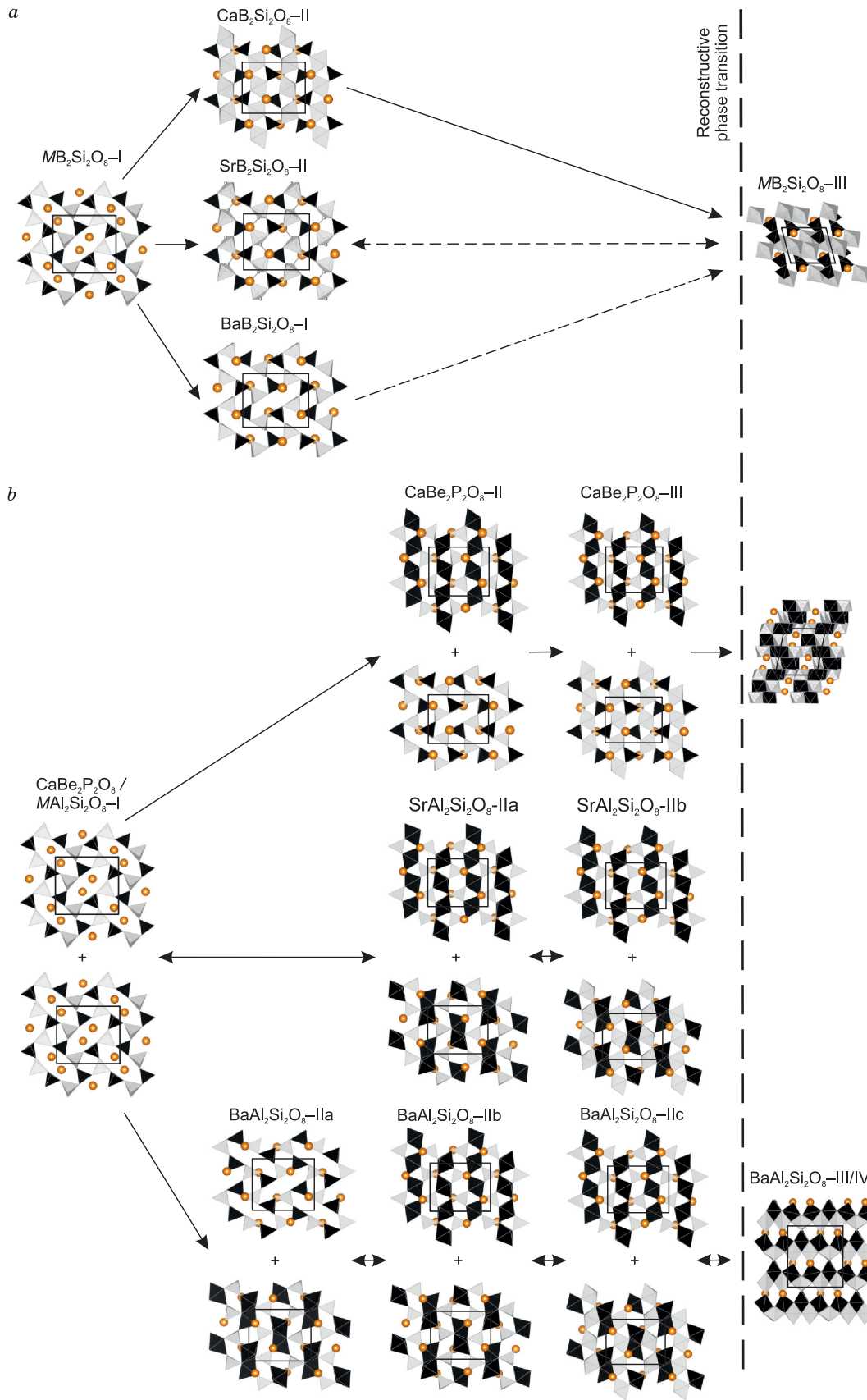


Fig. 6. The transformation schemes of feldspar-related minerals with the paracelsian topology under high pressure: *a* – orthorhombic minerals of the danburite group; *b* – monoclinic paracelsian, slawsonite and hurlbutite.

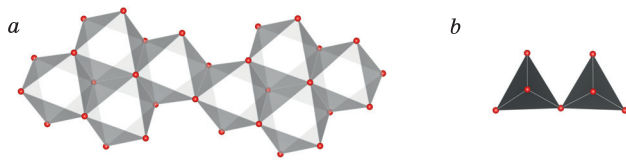


Fig. 7. Fragments of crystal structure of borosilicate FSPT members $MB_2Si_2O_8$ ($M = Ca, Sr, Ba$) after a reconstructive phase transition: *a* – a chain of SiO_6 octahedra; *b* – a dimer of BO_4 tetrahedra.

undergo phase transformations at substantially lower pressures (Gorelova et al., 2021b). This fact was recently confirmed by the example of layered minerals of the gadolinite group (Gorelova et al., 2023a). It is also worth mentioning that traditional ideas, that the increase in the cation size weakens the structure stability at high pressures (Neuhaus, 1964), do not work for feldspar-type structures with paracel-

sian topology, as it has been shown by the examples of boro- and aluminosilicates; therefore, beryllophosphates are expected to behave in a similar way.

MECHANISMS OF TO_5 POLYHEDRA FORMATION AT HIGH PRESSURES

The reasons why tetrahedra in silicates and silicate-like compounds are most often transformed directly into octahedra, bypassing the pentacoordinated state, are not completely clear. F. Liebau (1984) explained the absence of SiO_5 groups by the ionic nature of chemical bonds in silicates. It is generally accepted that ionic oxide compounds tend to form the densest packages of oxygen atoms, with cations filling the voids between them. Even under ambient conditions, there are many compounds, including silicates, whose crystal structures can be described as distorted hexagonal

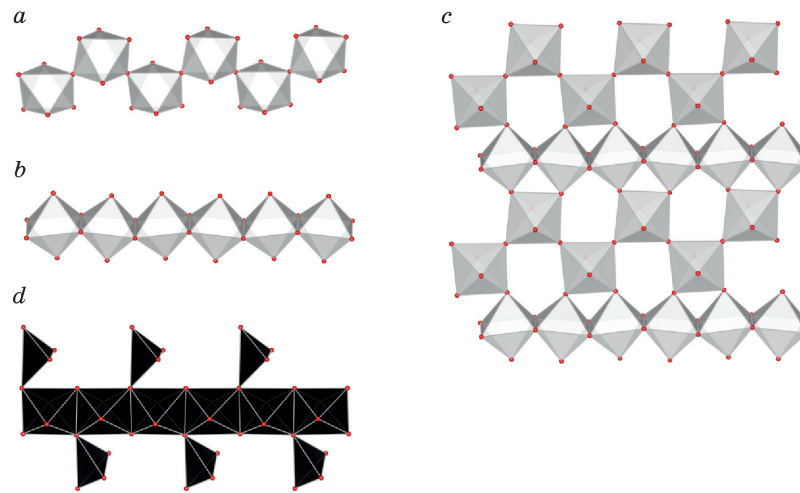


Fig. 8. Fragments of the crystal structure of paracelsian after a reconstructive phase transition: *a, b* – chains (fragments of a layer), *c* – a layer of SiO_6 octahedra, *d* – a chain of AlO_6 octahedra and distorted AlO_4 tetrahedra.

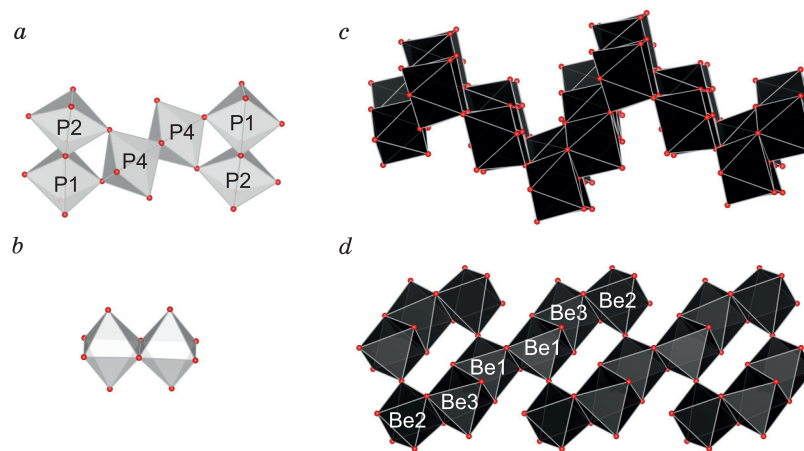


Fig. 9. Fragments of the crystal structure of hurlbutite after a reconstructive phase transition: *a* – a “cluster”, *b* – a dimer of PO_6 octahedra, *c* – a layer, *d* – a chain of BeO_6 octahedra.

(HCP) or cubic (CCP) closest packages (e.g., O atoms in the crystal structures of rutile, corundum, spinel, perovskite, etc.). However, the structures of the compounds considered in this work under ambient conditions are rather “loose”, but as the pressure increases, they tend to form the closest packages; this is achieved only after reconstructive phase transitions, accompanied by an increase in the coordination number to six. The intermediate phases containing TO_5 polyhedra ($T = \text{Si, Al, Be, P}$) consist of a rather complex combination of HCP and CCP fragments; this leads to the formation of complex five-fold voids, in addition to usual tetrahedral and octahedral.

The described above results of the study of a number of FSPT minerals show that the coordination polyhedra (especially SiO_5 , BeO_5 , PO_5) of different cations, rare for classical crystal chemistry, may not be as rare as it was previously considered. They can form as an intermediate phase between “loose” and “close packed” structures. SiO_5 polyhedra are known in high-pressure modifications of such minerals and synthetic compounds, as CaSi_2O_5 (Angel et al., 1996), brewsterite (Alberti et al., 1999), orthopyroxene (Finkelstein et al., 2015), diopside (Hu et al., 2017), coesite (Bykova et al., 2018), datolite (Gorelova et al., 2018), albite (Pakhomova et al., 2020), reedmergnerite (Gorelova et al., 2022). BeO_5 polyhedra are currently known only in hurlbutite described in this work, and PO_5 ones have also been obtained in a high-pressure modification of TiPO_4 (Bykov et al., 2016).

An interesting consequence of the appearance of such polyhedra in the structures of minerals is their acoustic “visibility”. Polymorphic modifications of minerals containing TO_5 polyhedra are significantly less dense comparing with octahedrally coordinated cations, typical for high-pressure structures; this results in a significant drop in sound velocities (Bykova et al., 2018). Another consequence of the appearance of TO_5 polyhedra may be the decay of solid solutions, due to the fact that some of the elements will not be able to be contained into pentacoordinated polyhedra. For example, changing in the coordination number of calcium from 6 to 8 causes some to form a carbonate-magnesium isomorphic series (e.g., calcite), while others do not (e.g., aragonite (Vereshchagin et al., 2021)). Similarly, crystal chemical fractionation of elements is likely to occur during the formation of high-pressure polymorphs with unusual structural groups.

CONCLUSIONS

The existence of the structures containing unusual coordination polyhedra has a significant effect on the density of matter, its elastic and plastic deformation, and therefore the density of the submerged lithospheric plate and its buoyancy in the Earth’s mantle (Hu et al., 2017). According to traditional ideas about the composition of the deep Earth’s interior, most minerals of the Earth’s crust are supposed to decompose into dense oxide or perovskite-like phases; this

requires overcoming kinetic barriers, and therefore high temperatures. However, the existence of phases containing SiO_5 polyhedra indicates the alternative ways of transforming minerals under high pressures and moderate temperatures.

ACKNOWLEDGEMENTS AND FUNDING

The author expresses her profound gratitude to A.V. Kasatkin for the provided sample, and to Dr. M.G. Krzhizhanovskaya (St. Petersburg State University) for conducting a high-temperature X-ray diffraction experiment for paracelsian, as well as Dr. O.S. Vereshchagin (St. Petersburg State University) for fruitful discussion and comprehensive assistance in the preparation of this manuscript. The author also cordially thanks a Corresponding Member of Russian Academy of Sciences Yu.N. Palyanov for his suggestion to prepare this review, as well as Dr. A.F. Shatsky and an anonymous reviewer for their help, constructive criticism and important suggestions which substantially improved the manuscript. High-temperature X-ray diffraction studies were carried out at the Resource Center “X-ray diffraction research methods” of St. Petersburg State University. This study was supported by the Russian Science Foundation (grant No. 22-77-10033).

REFERENCES

- Alberti, A., Sacerdoti, M., Quartieri, S., Vezzalini, G., 1999. Heating-induced phase transformation in zeolite brewsterite: new 4- and 5-coordinated (Si, Al) sites. *Phys. Chem. Miner.* 26, 181–186, doi: [10.1007/s002690050175](https://doi.org/10.1007/s002690050175).
- Angel, R.J., 1994. Feldspars at high pressure, in: Parsons, I. (Ed.), *Feldspars and Their Reactions*. Springer, Dordrecht, pp. 271–312, doi: [10.1007/978-94-011-1106-5_7](https://doi.org/10.1007/978-94-011-1106-5_7).
- Angel, R.J., Ross, N.L., Seifert, F., Fliervoet, T.F., 1996. Structural characterization of pentacoordinate silicon in a calcium silicate. *Nature*, 384, 441–444, doi: [10.1038/384441a0](https://doi.org/10.1038/384441a0).
- Angel, R.J., Sochalski-Kolbus, L.M., Tribaudino, M., 2012. Tilts and tetrahedra: the origin of the anisotropy of feldspars. *Am. Mineral.* 97, 765–778, doi: [10.2138/am.2012.4011](https://doi.org/10.2138/am.2012.4011).
- Bakakin, V.V., Rylov, G.M., Alekseev, V.I., 1974. Refinement of the crystal structure of horlbathite $\text{CaBe}_2\text{P}_2\text{O}_8$. *Sov. Phys. Crystallogr.* 19, 1283–1285.
- Bambauer, H.U., Nager, H.E., 1981. Gitterkonstanten und displazive Transformation synthetischer Erdalkaliefeldspate. I. System $\text{CaAl}_2\text{Si}_2\text{O}_8$ – $\text{SrAl}_2\text{Si}_2\text{O}_8$ – $\text{BaAl}_2\text{Si}_2\text{O}_8$. *Neues Jahrb. Miner. Abh.* 141, 225–239.
- Bokii, G.B., Borutskii, B.E., 2003. *Minerals. V.1. Framework Silicates, Issue 1. Silicates with Broken Frameworks. Feldspars* [in Russian]. Nauka, Moscow.
- Boruneta, C.R., Vennestrøm, P., Lundegaard, L.F., 2019. K-paracelsian ($\text{KAlSi}_3\text{O}_8 \cdot \text{H}_2\text{O}$) and identification of a simple building scheme of dense double-crankshaft zeolite topologies. *IUCrJ* 6, 66–71, doi: [10.1107/S2052252518016111](https://doi.org/10.1107/S2052252518016111).
- Brun, E., Ghose, S., 1964. Nuclear magnetic resonance spectrum of ^{11}B and B–Si order in danburite, $\text{CaB}_2\text{Si}_2\text{O}_8$. *J. Chem. Phys.* 40, 3031–3033.
- Bykov, M., Bykova, E., Hanfland, M., Liermann, H.-P., Kremer, R.K., Glaum, R., Dubrovinsky, L., van Smaalen, S., 2016. High-pressure phase transformations in TiPO_4 : a route to pentacoordinated

- phosphorous. *Angew. Chem.* 55, 15053–15057, doi: [10.1002/anie.201608530](https://doi.org/10.1002/anie.201608530).
- Bykova, E., Bykov, M., Černok, A., Tidholm, J., Simak, S.I., Hellman, O., Belov, M.P., Abrikosov, I.A., Liermann, H.-P., Hanfland, M., Prakupenka, V.B., Prescher, C., Dubrovinskaia, N., Dubrovinsky, L., 2018. Metastable silica high pressure polymorphs as structural proxies of deep Earth silicate melts. *Nat. Commun.* 9, 4789, doi: [10.1038/s41467-018-07265-z](https://doi.org/10.1038/s41467-018-07265-z).
- Chiari, G., Gazzoni, G., Craig, J.R., Gibbs, G.V., Louisnathan, S.J., 1985. Two independent refinements of the structure of paracelsian, $\text{BaAl}_2\text{Si}_2\text{O}_8$. *Am. Mineral.* 70, 969–974.
- Dal Bo, F., Hatert, F., Baijot, M., 2014. Crystal chemistry of synthetic $\text{M}^{2+}\text{Be}_2\text{P}_2\text{O}_8$ ($\text{M}^{2+} = \text{Ca}, \text{Sr}, \text{Pb}, \text{Ba}$). *Can. Mineral.* 52, 337–350, doi: [10.3749/canmin.52.2.337](https://doi.org/10.3749/canmin.52.2.337).
- Dana, E.S., 1892. Dana's system of mineralogy. John Wiley & Sons, New-York, pp. 490–492.
- Deer, W.A., Howie, R.A., Zussman, J., 2001. *Rock-Forming Minerals. Vol. 4A. Framework Silicates: Feldspars*. Geol. Soc., London.
- Dordević, T., 2011. $\text{Ba}(\text{ZnAsO}_4)_2 \cdot \text{H}_2\text{O}$, a non-centrosymmetric framework structure related to feldspar. *Eur. J. Miner.* 23, 437–447, doi: [10.1127/0935-1221/2011/0023-2100](https://doi.org/10.1127/0935-1221/2011/0023-2100).
- Dove, M.T., Cool, T., Palmer, D.C., Putnis, A., Salje, H., Winkler, B., 1993. On the role of Al–Si ordering in the cubic-tetragonal phase transitions of leucite. *Am. Mineral.* 78, 486–492.
- Dove, M.T., Pride, A.K.A., Keen, D.A., 2000. Phase transitions in tridymite studied using ‘Rigid Unit Mode’ theory, Reverse Monte Carlo methods and molecular dynamics simulations. *Min. Mag.* 64, 267–283.
- Downs, R.T., Yang, H., Hazen, R.M., Finger, L.W., Prewitt, C.T., 1999. Compressibility mechanisms of alkali feldspars; new data from reedmergnerite. *Am. Mineral.* 84, 333–340, doi: [10.2138/am-1999-0316](https://doi.org/10.2138/am-1999-0316).
- Finger, L.W., Hazen, R.M., 2000. Systematics of high-pressure silicate structures. *Rev. Mineral. Geochem.* 41, 123–155, doi: [10.2138/rmg.2000.41.5](https://doi.org/10.2138/rmg.2000.41.5).
- Finkelstein, G.J., Dera, P.K., Duffy, T.S., 2015. Phase transitions in orthopyroxene (En_{90}) to 49 GPa from single-crystal X-ray diffraction. *Phys. Earth Planet. Inter.* 244, 78–86, doi: [10.1016/j.pepi.2014.10.009](https://doi.org/10.1016/j.pepi.2014.10.009).
- Gorelova, L.A., Krzhizhanovskaya, M.G., Bubnova, R.S., 2012. Thermal expansion of borosilicate $\text{SrB}_2\text{Si}_2\text{O}_8$. *Fizika i Khimiya Stekla* 38 (S6), 872–875.
- Gorelova, L.A., Filatov, S.K., Krzhizhanovskaya, M.G., Bubnova, R.S., 2015. High-temperature behavior of danburite-like-borosilicates $\text{MB}_2\text{Si}_2\text{O}_8$ ($M = \text{Ca}, \text{Sr}, \text{Ba}$). *Phys. Chem. Glasses* 56, 189–196, doi: [10.13036/17533562.56.5.189](https://doi.org/10.13036/17533562.56.5.189).
- Gorelova, L.A., Pakhomova, A.S., Aprilis, G., Dubrovinsky, L.S., Krivovichev, S.V., 2018. Pentacoordinated silicon in the high-pressure modification of datolite, $\text{CaBSiO}_4(\text{OH})$. *Inorg. Chem. Front.* 5, 1653–1660, doi: [10.1039/C8Q100257F](https://doi.org/10.1039/C8Q100257F).
- Gorelova, L.A., Pakhomova, A.S., Krivovichev, S.V., Dubrovinsky, L.S., Kasatkin, A.V., 2019. High pressure phase transitions of paracelsian $\text{BaAl}_2\text{Si}_2\text{O}_8$. *Sci. Rep.* 9, 12652, doi: [10.1038/s41598-019-49112-1](https://doi.org/10.1038/s41598-019-49112-1).
- Gorelova, L.A., Pakhomova, A.S., Krzhizhanovskaya, M.G., Winkler, B., Krivovichev, S.V., Dubrovinsky, L.S., 2020. Pressure-induced phase transitions in danburite-type borosilicates. *J. Phys. Chem. C* 124, 26048–26061, doi: [10.1021/acs.jpcc.0c08616](https://doi.org/10.1021/acs.jpcc.0c08616).
- Gorelova, L.A., Pakhomova, A.S., Krzhizhanovskaya, M.G., Krivovichev, S.V., Dubrovinsky, L.S., Kasatkin, A.V., 2021a. Crystal structure evolution of slawsonite $\text{SrAl}_2\text{Si}_2\text{O}_8$ and paracelsian $\text{BaAl}_2\text{Si}_2\text{O}_8$ upon compression and decompression. *J. Phys. Chem. C* 125, 13014–13023, doi: [10.1021/acs.jpcc.0c08616](https://doi.org/10.1021/acs.jpcc.0c08616).
- Gorelova, L., Vereshchagin, O., Kasatkin, A., 2021b. Thermal expansion and polymorphism of slawsonite $\text{SrAl}_2\text{Si}_2\text{O}_8$. *Minerals* 11, 1150, doi: [10.3390/min11101150](https://doi.org/10.3390/min11101150).
- Gorelova, L., Pakhomova, A., Aprilis, G., Yin, Y., Laniel, D., Winkler, B., Krivovichev, S., Pekov, I., Dubrovinskaia, N., Dubrovinsky, L., 2022. Edge-sharing BO_4 tetrahedra and penta-coordinated silicon in the high-pressure modification of NaBSi_3O_8 . *Inorg. Chem. Front.* 9, 1735–1742, doi: [10.1039/D2Q100101B](https://doi.org/10.1039/D2Q100101B).
- Gorelova, L., Vereshchagin, O., Aslandukov, A., Aslandukova, A., Spiridonova, D., Krzhizhanovskaya, M., Kasatkin, A., Dubrovinsky, L., 2023a. Hydroxylherderite ($\text{Ca}_2\text{Be}_2\text{P}_2\text{O}_8(\text{OH})_2$) stability under extreme conditions (up to 750 °C/100 GPa). *J. Am. Ceram. Soc.* 106, 2622–2634, doi: [10.1111/jace.18923](https://doi.org/10.1111/jace.18923).
- Gorelova, L.A., Vereshchagin, O.S., Bocharov, S.N., Krivovichev, S.V., Zolotarev, A.A., Rassomakhin, M.A., 2023b. $\text{CaAl}_2\text{Si}_2\text{O}_8$ polymorphs: sensitive geothermometers and geospeedometers. *Geosci. Front.* 14, 101458, doi: [10.1016/j.gsf.2022.101458](https://doi.org/10.1016/j.gsf.2022.101458).
- Grew, E.S., Anovitz, L.M. (Eds.), 2002. *Boron: Mineralogy, Petrology and Geochemistry*. Rev. Mineral. 33.
- Griffen, D.T., Ribbe, P.H., Gibbs, G.V., 1977. The structure of slawsonite, a strontium analog of paracelsian. *Am. Mineral.* 62, 31–35.
- Henderson, M.B., 2021. Composition, thermal expansion and phase transitions in framework silicates: revisitation and review of natural and synthetic analogues of nepheline-, feldspar- and leucite-mineral groups. *Solids* 2, 1–49, doi: [10.3390/solids2010001](https://doi.org/10.3390/solids2010001).
- Hu, Y., Kiefer, B., Bina, C.R., Zhang, D., Dera, P.K., 2017. High-pressure $\gamma\text{-CaMgSi}_2\text{O}_6$: does penta-coordinated silicon exist in the Earth's Mantle? *Geophys. Res. Lett.* 44, 11340–11348, doi: [10.1002/2017GL075424](https://doi.org/10.1002/2017GL075424).
- Huong, L.T.-T., Otter, L.M., Haeger, T., Ullmann, T., Hofmeister, W., Weis, U., Jochum, K.P., 2016. A new find of danburite in the Luc Ten mining area, Vietnam. *Gems Gemmol.* 52, 393–401.
- Kimata, M., 1993. Crystal structure of KBSi_3O_8 isostructural with danburite. *Mineral. Mag.* 57, 157–164, doi: [10.1180/minmag.1993.057.386.15](https://doi.org/10.1180/minmag.1993.057.386.15).
- Klaska, R., Jarchow, O., 1977. KGaGe_2O_8 , ein Paracelsian-Typ mit einwertigem Kation. *Naturwiss.* 64, 92–93, doi: [10.1007/BF00437356](https://doi.org/10.1007/BF00437356).
- Krivovichev, S.V., 2020. Feldspar polymorphism: diversity, complexity, stability. *Zapiski Rossijskogo Mineralogicheskogo Obshchestva*, No. 149, 16–66.
- Krzhizhanovskaya, M.G., Gorelova, L.A., Bubnova, R.S., Pekov, I.V., Krivovichev, S.V., 2018. High-temperature crystal chemistry of layered calcium borosilicates: $\text{CaBSiO}_4(\text{OH})$ (datolite), $\text{Ca}_4\text{B}_3\text{Si}_3\text{O}_{15}(\text{OH})_5$ (‘bakerite’) and $\text{Ca}_2\text{B}_2\text{SiO}_7$ (synthetic analogue of okayamalite). *Phys. Chem. Mineral.* 45, 463–473, doi: [10.1007/s00269-017-0933-y](https://doi.org/10.1007/s00269-017-0933-y).
- Levin, E.M., Ugrinic, G.M., 1953. The system barium oxide–boric oxide–silica. *J. Res. Natl. Bur. Stand. (U.S.)* 51, 37–56.
- Liebau, F., 1984. Pentacoordinated silicon intermediate states during silicate condensation and decondensation. Crystallographic support. *Inorg. Chim. Acta* 89, 1–7, doi: [10.1016/S0020-1693\(00\)82422-6](https://doi.org/10.1016/S0020-1693(00)82422-6).
- Liu, Z., Chen, Z., Weng, L., Tu, B., Zhao, D., 2003. Synthesis and structure of a new aluminum germanate molecular sieve KAlGe_3O_8 . *J. Fudan Univ. (Nat. Sci.)* 42, 961–966.
- Matýšek, D., Jirásek, J., 2016. Occurrences of slawsonite in rocks of the Teschenite association in the Podbeskydi piedmont area (Czech Republic) and their petrological significance. *Can. Mineral.* 54, 1129–1146, doi: [10.3749/canmin.1500101](https://doi.org/10.3749/canmin.1500101).
- McCaughey, R.A., 2000. Polymorphism and dielectric electric properties of Ba- and Sr-containing feldspars. *J. Mater. Sci.* 35, 3939–3942, doi: [10.1023/A:1004802002579](https://doi.org/10.1023/A:1004802002579).
- Mookherjee, M., Mainprice, D., Maheshwari, K., Heinonen, O., Patel, D., Hariharan, A., 2016. Pressure induced elastic softening in framework aluminosilicate-albite ($\text{NaAlSi}_3\text{O}_8$). *Sci. Rep.* 6, 34815, doi: [10.1038/srep34815](https://doi.org/10.1038/srep34815).
- Mrose, M.E., 1952. Hurlbutite, $\text{CaBe}_2(\text{PO}_4)_2$, a new mineral. *Am. Mineral.* 37, 931–940.
- Neuhaus, 1964. Synthese Strukturverhalten + Valenzzustände der anorganischen Materie im Bereich hoher + hochster Drucke. *Chimia* 18, 93.

- Pakhomova, A.S., Bykova, E., Bykov, M., Glazyrin, K., Gasharova, B., Liermann, H.P., Mezouar, M., Gorelova, L.A., Krivovichev, S.V., Dubrovinsky, L., 2017. A closer look into close packing: pentacoordinated silicon in the high-pressure polymorph of danburite. *IUCrJ.* 4, 671–677, doi: [10.1107/S2052252517010612](https://doi.org/10.1107/S2052252517010612).
- Pakhomova, A., Aprilis, G., Bykov, M., Gorelova, L., Krivovichev, S., Belov, M.P., Abrikosov, I.A., Dubrovinsky, L., 2019. Penta- and hexa-coordinated beryllium and phosphorus in high-pressure modifications of $\text{CaBe}_2\text{P}_2\text{O}_8$. *Nat. Commun.* 10, 2800, doi: [10.1038/s41467-019-10589-z](https://doi.org/10.1038/s41467-019-10589-z).
- Pakhomova, A., Simonova, D., Koemets, I., Koemets, E., Aprilis, G., Bykov, M., Gorelova, L., Fedotenko, T., Prakapenka, V., Dubrovinsky, L., 2020. Polymorphism of feldspars above 10 GPa. *Nat. Commun.* 11, 2721, doi: [10.1038/s41467-020-16547-4](https://doi.org/10.1038/s41467-020-16547-4).
- Palmer, D.C., Dove, M.T., Ibberson, R.M., Powell, B.M., 1997. Structural behavior, crystal chemistry, and phase transitions in substituted leucite: High resolution neutron powder diffraction studies. *Am. Mineral.* 82, 16–29, doi: [10.2138/am-1997-1-203](https://doi.org/10.2138/am-1997-1-203).
- Parsons, I., 1994. *Feldspars and Their Reactions*. Springer, Dordrecht, doi: [10.1007/978-94-011-1106-5](https://doi.org/10.1007/978-94-011-1106-5).
- Pautov, L.A., Agakhanov, A.A., Sokolova, E., Hawthorne, F.C., 2004. Maleevite, $\text{BaB}_2\text{Si}_2\text{O}_8$, and pekovite, $\text{SrB}_2\text{Si}_2\text{O}_8$, new mineral species from the Dara-i-Pioz Alkaline Massif, northern Tajikistan: description and crystal structure. *Can. Mineral.* 42, 107–119, doi: [10.2113/gscanmin.42.1.107](https://doi.org/10.2113/gscanmin.42.1.107).
- Pautov, L.A., Agakhanov, A.A., Pekov, I.V., Karpenko, V.Yu., 2022. “Quartz Lumps” in the Darai-Piyoz alkaline massif (Tajikistan): on problems of their genesis and the cesium accumulation. *Zapiski Rossiiskogo Mineralogicheskogo Obshchestva* 151 (4), 102–122.
- Qin, N., Krzmann, M.M., Meden, A., Suvorov, D., 2009. Structural investigation of $\text{K}_x\text{Ba}_{1-x}\text{Ga}_{2-x}\text{Ge}_{2+x}\text{O}_8$ solid solutions using the X-ray Rietveld method. *J. Solid State Chem.* 182, 1666–1672, doi: [10.1016/j.jssc.2009.03.004](https://doi.org/10.1016/j.jssc.2009.03.004).
- Rao, C., Wang, R., Hatert, F., Gu, X., Ottolini, L., Hu, H., Dong, C., Dal Bo, F., Baijot M., 2014. Strontiohurlbutite, $\text{SrBe}_2(\text{PO}_4)_2$, a new mineral from Nanping No. 31 pegmatite, Fujian Province, Southeastern China. *Am. Mineral.* 99, 494–499, doi: [10.2138/am.2014.4547](https://doi.org/10.2138/am.2014.4547).
- Ratkin, V.V., Eliseeva, O.A., Pandian, M.S., Orekhov, A.A., Mohapatra, M., Vishnu Priya, S.K., 2018. Stages and formation conditions of productive mineral associations of the Dalnegorsk borosilicate deposit, Sikhote Alin. *Geol. Ore Deposits* 60, 672–684, doi: [10.1134/S107570151808007X](https://doi.org/10.1134/S107570151808007X).
- Shannon, R.D., 1976. Revised effective ionic radii and systematic studies of interatomic distances in halides and chalcogenides. *Acta Cryst. A* 32, 751–767, doi: [10.1107/S0567739476001551](https://doi.org/10.1107/S0567739476001551).
- Shepard, C.U., 1839. Notice of danburite, a new mineral species. *Am. J. Sci. Arts* 35, 137–139.
- Sleight, A.W., 1995. Thermal contraction. *Endeavor* 19, 64–68.
- Smith, J.V., 1978. Enumeration of 4-connected 3-dimensional nets and classification of framework silicates. II. Perpendicular and near-perpendicular linkages from 4.82, 3.122 and 4.6.12 nets. *Am. Mineral.* 63, 960–969.
- Smith, J.V., Rinaldi, F., 1962. Framework structures formed from parallel four- and eight-membered rings. *Mineral. Mag.* 33, 202–212, doi: [10.1180/minmag.1962.033.258.03](https://doi.org/10.1180/minmag.1962.033.258.03).
- Smith, J.V., Brown, W.L., 1988. *Feldspar Minerals. Vol. 1. Crystal Structures, Physical, Chemical and Microstructural Properties*. Springer Verlag, Berlin Heidelberg.
- Spencer, L.J., 1942. Barium feldspars, (celsian and paracelsian) from Wales. *Mineral. Mag.* 26, 231–245, doi: [10.1180/minmag.1942.026.178.01](https://doi.org/10.1180/minmag.1942.026.178.01).
- Sugiyama, K., Takéuchi, Y., 1985. Unusual thermal expansion of a B–O bond in the structure of danburite $\text{CaB}_2\text{Si}_2\text{O}_8$. *Z. Kristallogr.* 173, 293–304, doi: [10.1524/zkri.1985.173.3-4.293](https://doi.org/10.1524/zkri.1985.173.3-4.293).
- Tacconi, E., 1905. Di un silicato di alluminio e bario dei calcefirri di Candoglia in valle del Toce. *Rendiconti Reale Istituto Lombardo di Scienze e Lettere (Milano)* 38, 636–643.
- Tagai, T., Hoshi, T., Suzuki, M., Kato, A., Matsubara, S., 1995. A new modification of slawsonite, $\text{SrAl}_2\text{Si}_2\text{O}_8$. *Z. Kristallogr.* 210, 741–745, doi: [10.1524/zkri.1995.210.10.741](https://doi.org/10.1524/zkri.1995.210.10.741).
- Tasáryová, Z., Fryda, J., Janousek, V., Racek, M., 2014. Slawsonite–celsian–hyalophane assemblage from a picrate sill (Prague Basin, Czech Republic). *Am. Mineral.* 99, 2272–2279, doi: [10.2138/am-2014-4770](https://doi.org/10.2138/am-2014-4770).
- Tripathi, A., Parise, J.B., 2002. Hydrothermal synthesis and structural characterization of the aluminogermanate analogues of JBW, montesommaite, analcime and paracelsian. *Micropor. Mesopor. Mater.* 52, 65–78, doi: [10.1016/S1387-1811\(02\)00270-6](https://doi.org/10.1016/S1387-1811(02)00270-6).
- Vereshchagin, O.S., Frank-Kamenetskaya, O.V., Kuz'mina, M.A., Chernyshova, I.A., Shilovskikh, V.V., 2021. Effect of magnesium on monohydrocalcite formation and unit-cell parameters. *Am. Mineral.* 106, 1294–1305, doi: [10.2138/am-2021-7673](https://doi.org/10.2138/am-2021-7673).
- Zabukovec-Logar, N., Mrak, M., Kaučič, V., 2001. Synthesis and structures of two ammonium zinc gallophosphates: analcime and paracelsian analogs. *J. Solid State Chem.* 156, 480–486, doi: [10.1006/jssc.2000.9027](https://doi.org/10.1006/jssc.2000.9027).